ISSN: 2688-8645

Experimental Study on Ripple Characteristics Testing and Adaptability of Electric Vehicle High-Voltage Systems

Chunjiang Meng, Songmao Wei and Guang Shi *

CATARC Engineering Research Institute (Tianjin) Co., Ltd., Tianjin, 300300, China

* Corresponding Author: Guang Shi

Abstract

Voltage ripple in the high-voltage DC bus of electric vehicles is a key factor affecting system stability and component lifetime. This study built a chassis dynamometer test platform and tested the high-voltage ripple of a production battery electric vehicle under different SOC ranges, driving modes, and load conditions. Test data show that ripple peak-to-peak values are generally below 10 Vpp under steady-state cruising conditions, while they rise markedly under dynamic conditions; the transient peak reaches 44.12 Vpp in 0-100 km/h hard acceleration with Sport+ mode, and drops to 25.93 Vpp in anti-motion-sickness mode. Ripple levels differ little across SOC ranges. Based on the test data, this paper analyzes the ripple generation mechanism and discusses suppression strategies, providing a reference for the optimal design of high-voltage systems.

Keywords

Electric Vehicles; High-voltage System; Voltage Ripple; Vehicle Test; Ripple Suppression.

1. Introduction

Driven by the global energy transition and carbon-neutrality goals, the electric vehicle (EV) industry has been growing explosively. Unlike conventional fuel vehicles, EVs carry a complex high-voltage (HV) electrical system that integrates multiple power electronic components, including the traction battery, motor controller, DC/DC converter, on-board charger (OBC), air-conditioning compressor and PTC heater [1]. These components are interconnected through the HV DC bus, forming a complex distributed power-electronics network. However, owing to the high-frequency switching of power devices in converters and the severe dynamic changes of load current, voltage ripple on the HV bus is inevitable [2].

Voltage ripple refers to the AC component superimposed on the DC voltage, and its magnitude is usually measured by the peak-to-peak value (Vpp). HV bus ripple affects vehicle reliability in several aspects. First, ripple current flowing through the battery internal resistance generates additional Joule heat, which raises the battery pack temperature, accelerates battery aging and shortens its service life [3]. Second, high-frequency ripple components produce electromagnetic interference (EMI) by radiation and conduction, disturbing on-board sensors, wireless communication modules and infotainment systems [4]. More seriously, excessive ripple may cause burning or welding of HV relay contacts, leading to serious electrical safety accidents [5].

In recent years, extensive research has been conducted on HV ripple. Liu and Lai pointed out that in fuel cell power systems, low-frequency current ripple can significantly reduce the output capability of the fuel cell and even trigger overcurrent protection [3]. Kabalo et al experimentally validated the effectiveness of high-voltage-ratio, low-input-current-ripple converters in hybrid fuel cell/supercapacitor systems [6]. Yan et al compared domestic and international standards, proposed a ripple test procedure for HV components, and verified it on several DC/DC converters [7]. Liu et al proposed a ripple immunity test method for electric

ISSN: 2688-8645

drive systems based on real-vehicle operating data, to verify component adaptability under complex ripple conditions [8]. However, existing studies mostly focus on testing or simulation of a single component; ripple testing at the complete-vehicle level under full operating conditions remains scarce, and vehicle-level ripple test data are particularly rare.

To this end, this paper carries out full-vehicle HV ripple tests on a production battery electric vehicle. The tests cover different SOC ranges, driving modes, dynamic operating conditions and auxiliary loads, and the collected HV bus ripple data are analyzed to identify the influence of each factor, providing a reference for optimized system design.

2. Generation Mechanism and Effects of High-Voltage Ripple

2.1. Ripple Generation Mechanism

The ripple sources on the HV DC bus of an EV are complex and can be divided into two categories: switching ripple and load-dynamic ripple.

The first is switching ripple, which is the dominant source. The core of every power converter in the HV system, such as the motor controller, DC/DC converter and OBC, is an inverter or rectifier bridge composed of IGBT or MOSFET devices. These switches operate at frequencies of several kilohertz, converting DC power into AC power or vice versa. In this process, the input current inevitably contains high-frequency AC components related to the switching frequency [9]. According to Kirchhoff's laws, when these AC ripple currents flow through the equivalent impedance of the HV bus, a corresponding voltage ripple is produced on the bus. Since different components switch at different frequencies, these ripple components superimpose on the bus, forming a complex spectral distribution.

The second is load-dynamic ripple. During hard acceleration, hard deceleration, or the switching in/out of high-power loads such as the air conditioner and the PTC heater, the load current changes dramatically within a very short time. Owing to the internal resistance of the traction battery and the bus capacitance, such sudden current changes cannot be absorbed instantaneously, resulting in large transient fluctuations of the bus voltage [10]. These fluctuations are usually low in frequency but large in amplitude, and are the main contributor to the time-domain ripple Vpp. For example, under hard acceleration, the input current of the motor controller may surge from tens of amperes to hundreds of amperes within a few hundred milliseconds, which inevitably causes an instantaneous voltage sag and recovery on the bus, producing a large voltage fluctuation.

2.2. Effects of Voltage Ripple on the System

The presence of voltage ripple poses a potential threat to the reliability and lifetime of the HV system.

First, it accelerates battery aging. Ripple current flowing through the battery internal resistance generates additional losses, which are ultimately converted into heat. Over long-term cycling, ripple current raises the battery temperature, promotes SEI film thickening and increases the internal resistance, thereby accelerating capacity fade. Lithium-ion batteries are particularly sensitive to current fluctuations, and excessive ripple can damage the microstructure of the electrodes.

Second, it causes electromagnetic interference. High-frequency voltage ripple is conducted to various components through the power lines and also radiates through space, disturbing nearby low-level signal circuits. For example, ripple may interfere with the sampling accuracy of the battery management system (BMS), causing voltage and current measurement errors, and may even affect the sensor signals of the advanced driver assistance system (ADAS), compromising driving safety [11].

ISSN: 2688-8645

Third, it leads to overheating and failure of components. For the bus support capacitor, ripple current is the main source of heat. The capacitor lifetime has an exponential relationship with its core temperature; excessive ripple current sharply raises the core temperature and greatly shortens its service life [12]. In addition, ripple may cause contact vibration of the HV contactor, leading to contact erosion and, in severe cases, contact welding, resulting in a serious safety accident in which the circuit cannot be disconnected.

3. Test Scheme Design

3.1. Test Scheme and Operating Conditions

To comprehensively cover the real-world operating scenarios of the vehicle, a multi-dimensional test matrix was designed.

SOC range division: to verify the performance of the HV system at different battery levels, the battery SOC was divided into three ranges: high SOC (60%-90%), medium SOC (30%-60%) and low SOC (10%-30%), covering most usage scenarios from fully charged to low battery.

Vehicle operating conditions: steady-state and dynamic conditions were designed according to different driving states, including:

Steady-state conditions: cruising at 100 km/h; cruising at 80 km/h on a 10% grade;

Dynamic conditions: 0-100 km/h hard acceleration; 80-120 km/h overtaking; 120-0 km/h emergency braking; 120-40 km/h coasting;

Static condition: charging while parked.

Driving mode and load combinations: to investigate the influence of control strategies and auxiliary loads, the tests covered three driving modes (Sport+, Comfort and anti-motion-sickness) and two energy-recovery modes (100% and 0%). In addition, under each operating condition, various load states were tested, including the A/C switching in/out, the PTC heater switching in/out, A/C on, PTC on, and both the A/C and the heater off, totaling 130 test cases.

3.2. Test System

The tests were performed on a chassis dynamometer equipped with an environmental chamber, ensuring that the vehicle load corresponded to actual road conditions. Voltage ripple was acquired with a high-precision oscilloscope using a high-voltage differential probe connected to the HV bus, with AC coupling to remove the DC component so as to capture the AC ripple accurately. The test channels simultaneously recorded the HV voltage, compressor current and PTC current, to analyze the correspondence between load changes and ripple [13].

4. Test Results and Analysis

4.1. Overall Test Results

A total of 130 test cases were executed, covering combinations of SOC ranges, driving modes, dynamic conditions and auxiliary loads. The time-domain ripple Vpp data show that the ripple under steady-state cruising was generally below 10 Vpp, while under highly dynamic conditions such as hard acceleration and overtaking the ripple amplitude increased significantly, with the highest transient peak reaching 44.12 Vpp (in the 0-100 km/h hard acceleration with Sport+ mode). During the tests, no obvious ripple-induced anomalies were observed in the simultaneously recorded HV voltage, compressor and PTC current channels.

Overall, the distribution of the time-domain ripple Vpp shows a clear dependence on operating conditions. Under steady-state cruising, the ripple was generally low, mostly below 10 Vpp; under highly dynamic conditions such as hard acceleration and overtaking, the ripple amplitude rose significantly, with the highest transient peak reaching 44.12 Vpp. This is

ISSN: 2688-8645

consistent with the mechanism analysis above, i.e., large dynamic changes in current are the main cause of large ripple.

4.2. Effect of Driving Mode on Ripple

The test data of the two dynamic conditions, hard acceleration and overtaking, are extracted below to compare the ripple under different control strategies.

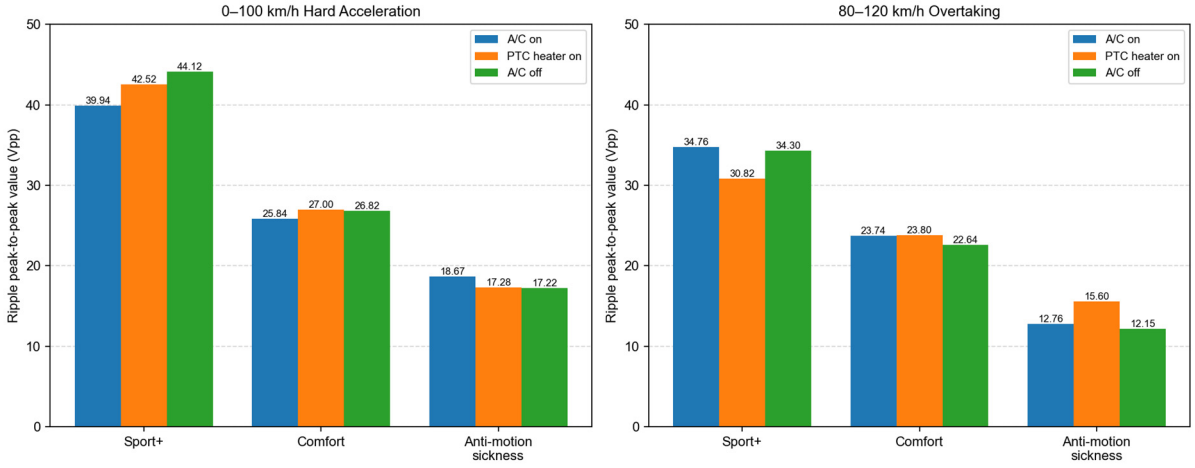


Figure 1. Comparison of HV ripple between hard acceleration and overtaking under different driving modes (Vpp, SOC 60%-90%)

As shown in Fig. 1 (left) and Table 1, under the 0-100 km/h hard acceleration condition, Sport+ mode produced the highest ripple peak, reaching 44.12 Vpp in the SOC 60%-90% range with the A/C off. This is because Sport+ mode gives the most aggressive power response, the largest rate of change of the accelerator pedal opening, and extremely fast variation of the motor output torque, thereby causing severe fluctuations of the bus current. By contrast, the ripple peak dropped to 25.84-27.00 Vpp in Comfort mode and further to 17.22-18.67 Vpp in anti-motion-sickness mode, about 60% lower than in Sport+ mode. The main reason is that the anti-motion-sickness mode smooths the rate of change of the motor current by optimizing the slope of the torque response, thereby effectively suppressing the voltage ripple caused by abrupt load changes. This rule also holds in other SOC ranges: across all SOC ranges and load combinations, the highest ripple peak of the anti-motion-sickness mode was 25.93 Vpp, still significantly lower than the 44.12 Vpp of Sport+ mode.

Table 1. Ripple peak-to-peak values under different driving modes in the 0-100 km/h hard acceleration condition (Vpp, SOC 60%-90%)

Driving Mode	A/C on	PTC Heater on	A/C off
Sport+	39.94	42.52	44.12
Comfort	25.84	27.00	26.82
Anti-motion-ickness	18.67	17.28	17.22

The overtaking condition shows the same trend (Fig. 1 (right) and Table 2): in the SOC 60%-90% range, the ripple peak of Sport+ mode was 30.82-34.76 Vpp, while that of the anti-motion-sickness mode was only 12.15-15.60 Vpp, a reduction of more than 50%; over the full SOC range, the peaks of the two modes were 35.49 Vpp and 16.05 Vpp, respectively. This indicates that optimizing the VCU torque filtering algorithm can reduce dynamic ripple without additional hardware cost, representing a low-cost software optimization direction.

ISSN: 2688-8645

Table 2. Ripple peak-to-peak values under different driving modes in the 80-120 km/h overtaking condition (Vpp, SOC 60%-90%)

Driving Mode	A/C on	PTC Heater on	A/C off
Sport+	34.76	30.82	34.30
Comfort	23.74	23.80	22.64
Anti-motion-ickness	12.76	15.60	12.15

4.3. Effect of SOC Range on Ripple

Averaging the time-domain ripple Vpp over all 41 operating conditions in each SOC range shows that the average ripple increases only slightly from 15.59 Vpp to 16.56 Vpp as the SOC decreases from high to low, an increase of less than 1 Vpp. This indicates that the HV system of this vehicle model maintains stable output characteristics over the entire SOC range.

This benefit mainly comes from the wide voltage adaptation range of the motor controller: whether the battery is at a high voltage (fully charged) or a low voltage (depleted), the converter maintains stable control by adjusting the PWM duty cycle, keeping the ripple characteristics consistent.

4.4. Analysis of Typical Operating Conditions

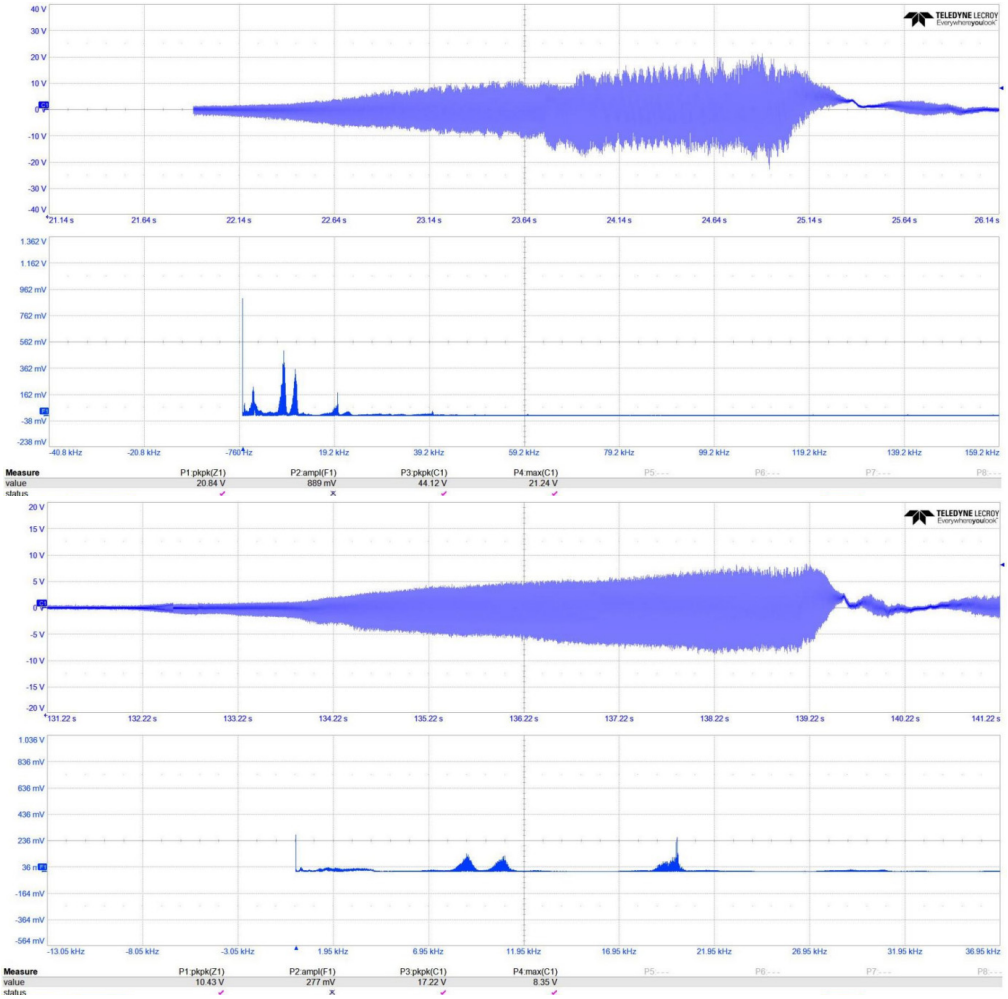


Figure 2. DC-bus voltage ripple waveforms under the 0-100 km/h hard acceleration condition with different driving modes (upper: Sport+ mode; lower: anti-motion-sickness mode)

To show the time-domain characteristics of the ripple more intuitively, typical raw waveforms of the two dynamic conditions (hard acceleration and overtaking) and of the steady-state

ISSN: 2688-8645

cruising condition under different driving modes were selected for comparative analysis. All waveforms below are time-domain waveforms of the HV bus voltage (AC coupled) together with their spectra, tested at SOC 60%-90%.

As shown in Fig. 2, during the 0-100 km/h hard acceleration, the bus ripple of both modes gradually increases with the driving current, but the amplitudes differ significantly. In Sport+ mode (upper), full throttle makes the motor current rise rapidly and the ripple envelope keeps widening, reaching a Vpp of 44.12 Vpp over the whole acceleration process, with the spectral energy concentrated mainly in the low-frequency band below 20 kHz; in anti-motion-sickness mode (lower), the smoothing of the torque-response slope limits the rate of change of the bus current, and the Vpp of the same acceleration process is only 17.22 Vpp, with a much narrower waveform envelope. The two sets of waveforms confirm the significant influence of the driving mode on load-dynamic ripple in both the time and frequency domains.

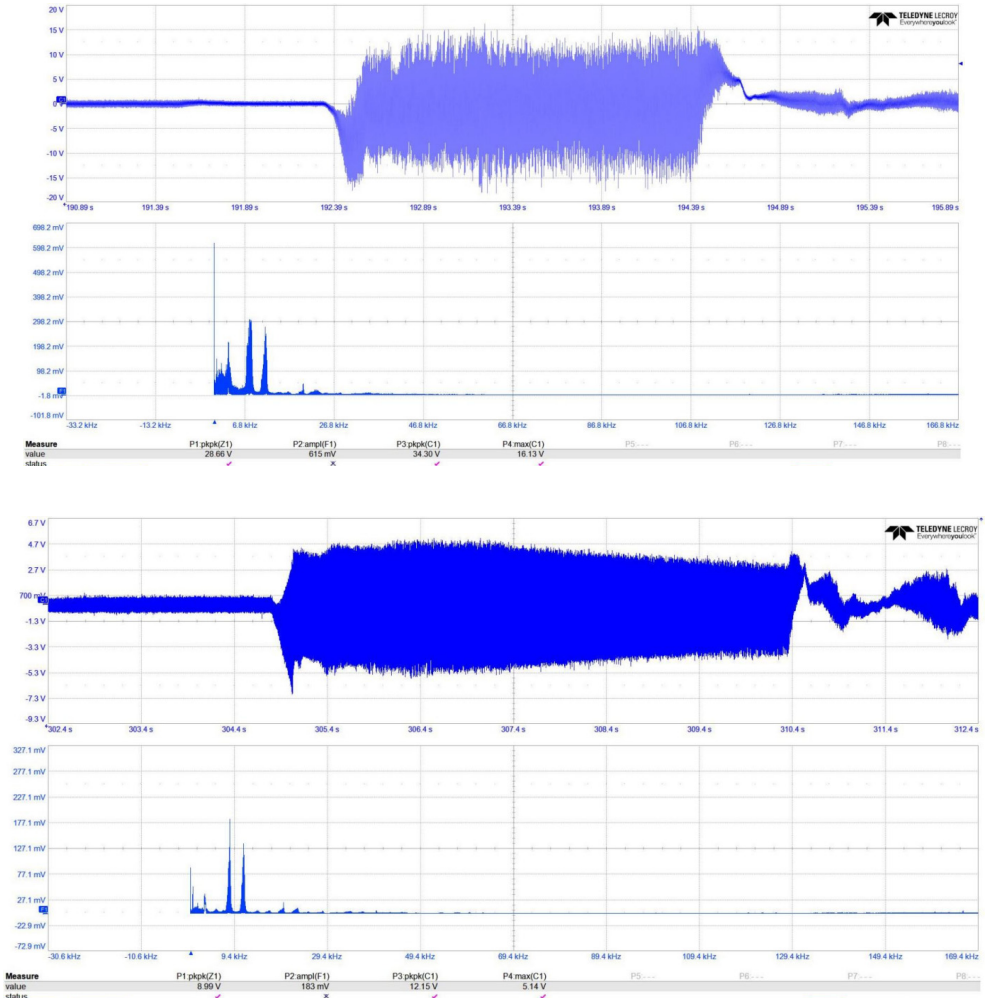


Figure 3. DC-bus voltage ripple waveforms under the 80-120 km/h overtaking condition with different driving modes (upper: Sport+ mode; lower: anti-motion-sickness mode)

Fig. 3 shows the comparative waveforms of the 80-120 km/h overtaking condition. In Sport+ mode (upper), the ripple Vpp reaches 34.30 Vpp during the whole overtaking process; in anti-motion-sickness mode (lower), the same process is only 12.15 Vpp, less than 40% of the Sport+ value. It can also be observed that in anti-motion-sickness mode the ripple envelope widens much more slowly as the vehicle speed rises, indicating that the smoothing of the torque change rate directly translates into a reduction of the bus voltage fluctuation. This is consistent with the statistical results in Table 2.

ISSN: 2688-8645

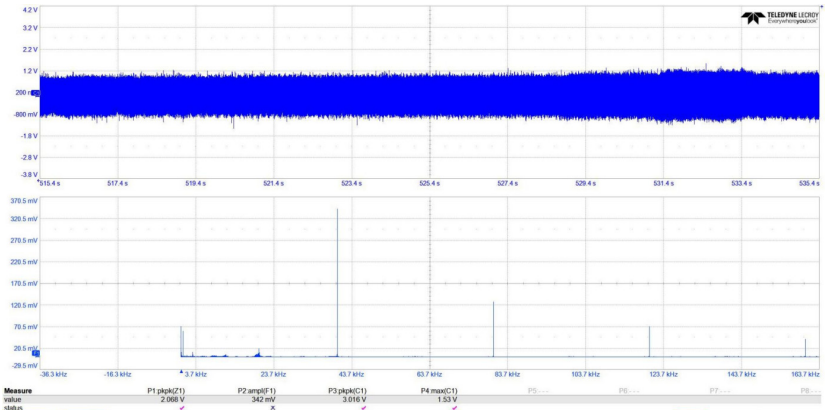


Figure 4. DC-bus voltage ripple waveform under the steady-state 100 km/h cruising condition (SOC 60%-90%, A/C on)

As a comparison, Fig. 4 shows the waveform under the steady-state 100 km/h cruising condition (A/C on). Throughout the recorded period, the bus voltage exhibits only high-frequency switching ripple of very small amplitude, with no obvious low-frequency fluctuation; the Vpp is only 3.02 Vpp, and the spectrum shows discrete spectral lines at the switching frequency. This contrasts sharply with the dynamic-condition data in Tables 1 and 2, indicating that the system power flow is stable in steady state and that the switching ripple is effectively suppressed by the input filter, which also explains why the ripple test results are generally good under steady-state conditions.

5. Discussion on Ripple Suppression Strategies

Based on the test results, the mechanism analysis and existing research, the optimization directions for HV system ripple suppression are discussed in the following three aspects.

5.1. Passive Filter Network Optimization

Passive filtering is the most basic and commonly used ripple suppression method. Adding X capacitors or LC filter networks to the HV bus can effectively absorb high-frequency switching ripple [14]. The tests showed that the high-frequency ripple was always well controlled, thanks to the good EMC filter design of the original vehicle. However, as switching frequencies continue to rise, the filter parameters can be further optimized in the future to achieve a better balance among size, cost and filtering performance.

5.2. Active Control and Load Smoothing

The test data show that software strategy has a great influence on ripple, as demonstrated by the substantial ripple reduction in anti-motion-sickness mode. In the future, a smarter torque-smoothing algorithm can be introduced in the vehicle control unit (VCU) to pre-filter the driver's accelerator input and limit the maximum torque change rate. Meanwhile, for the switching-in of high-power loads such as the A/C and the PTC heater, a soft-start strategy can be adopted to ramp the current up slowly, thereby avoiding the voltage impact caused by hard switching.

5.3. Topology and Converter Optimization

At the component level, DC/DC converters and OBCs using interleaved parallel technology can effectively cancel the input current ripple. For example, in a two-phase interleaved Boost converter, the input current ripples of the two phases cancel each other, greatly reducing the interference injected into the bus [15]. In addition, using supercapacitors or active buffer circuits to absorb transient power fluctuations is also an effective solution for suppressing large dynamic ripple. The integrated onboard charger topology proposed by Zhang et al exploits the

ISSN: 2688-8645

redundant capability of the charger to actively filter the bus ripple, achieving multiple functions with a single converter [16].

6. Conclusion and Outlook

This study conducted a full-operating-condition experimental investigation of the HV ripple characteristics of a battery electric vehicle. Based on the test data, the following observations and conclusions are drawn:

First, among the 130 condition combinations covered by the tests, the ripple Vpp under steady-state cruising was generally below 10 Vpp, while a highest transient peak of 44.12 Vpp occurred under highly dynamic conditions (0-100 km/h hard acceleration, Sport+ mode). The ripple levels differed little across SOC ranges, and no obvious shift of ripple characteristics was observed within the tested battery range.

Second, the ripple amplitude is closely related to the operating condition: dynamic conditions produce much higher ripple than steady-state conditions, and the driving mode has a significant influence. Sport+ mode, with its fast torque response, gives the highest ripple peak, while the anti-motion-sickness mode reduces the peak from 44.12 Vpp to 25.93 Vpp by smoothing the torque-response slope.

Third, the SOC state has very little influence on the overall ripple level, indicating that the system can maintain stable power quality over the entire battery range.

In the future, as EVs evolve toward 800 V high-voltage platforms and power density keeps increasing, the HV ripple problem will face new challenges. Follow-up research can further focus on the ripple coupling effect when multiple components operate in parallel and on the new characteristics of high-frequency ripple introduced by wide-bandgap devices such as SiC, thereby providing more comprehensive theoretical and experimental support for the design of next-generation HV systems.

References

[1] Lou, J. F., & Liu, G. C. (2020). Design challenges of high voltage DC bus system for new energy vehicles. Auto Electric, (12), 30–36. (in Chinese)

[2] Liu, Q. Q. (2018). Bidirectional DC converter for electric vehicles and single-phase charging secondary ripple suppression method [Master's thesis]. Tianjin University, China. (in Chinese)

[3] Liu, C., & Lai, J. (2007). Low frequency current ripple reduction technique with active control in a fuel cell power system with inverter load. IEEE Transactions on Power Electronics, 22(4), 1429–1436. https://doi.org/10.1109/TPEL.2007.900514.

[4] Yang, W. R., Luan, J. L., Liu, C., et al. (2021). Research on electromagnetic interference and suppression of three-in-one charging system assembly. Experimental Technology & Management, 38(9), 143–148. (in Chinese)

[5] Zhao, L. X., Pan, Q. X., & Si, K. (2024). Research on high-voltage ripple test method for electric vehicle electric drive system. China High-Tech, (12), 85–87. (in Chinese)

[6] Kabalo, M., Paire, D., Blunier, B., et al. (2012). Experimental validation of high-voltage-ratio low-input-current-ripple converters for hybrid fuel cell supercapacitor systems. IEEE Transactions on Vehicular Technology, 61(8), 3430–3440. https://doi.org/10.1109/TVT.2012.2203360.

[7] Yan, Z. B., Si, K., & Zhao, L. X. (2023). Experimental analysis of voltage ripple generated by high-voltage system components of electric vehicles. Auto Parts, (10), 30–33. (in Chinese)

[8] Liu, J. C., Shan, X. P., Zhao, L. X., et al. (2021). Analysis of voltage ripple characteristics of high-voltage internal network of new energy vehicles. Auto Sci-tech, (6), 100–105. (in Chinese)

[9] Cao, X. (2022). Research on capacitor ripple current suppression of dual-motor controller. Mechanical and Electrical Information, (6), 5–10. (in Chinese)

[10] Ni, M. H. (2021). Research on multilevel voltage-balancing DC-DC converter for high-voltage DC urban rail traction power supply system [Master's thesis]. Beijing Jiaotong University, China. (in Chinese)

[11] Willmann, B., Rinkleff, T., Obholz, M., et al. (2015). Automotive industry's EMC requirements for voltage ripple in the high-voltage system of electrical vehicles. In Proceedings of the 2015 IEEE International Symposium on Electromagnetic Compatibility (EMC) (pp. 673–678). https://doi.org/10.1109/ISEMC.2015.7256884.

[12] Liu, H. D., Zhang, Z. X., Chen, T., et al. (2021). Sub-resonance mechanism and suppression strategy of traction power electronic transformer. Journal of the China Railway Society, 43(6), 45–53. (in Chinese)

[13] Xiao, H. H., Zhou, C. L., Guo, Q., et al. (2021). Sector optimization modulation strategy of current-source rectifier for improving DC-link current ripple. Transactions of China Electrotechnical Society, 36(24), 5250–5260. (in Chinese)

[14] Niu, C. K., & Sun, X. B. (2025). Development of test system for bus self-generated high-voltage ripple of electric vehicle motor controller. Agricultural Equipment and Vehicle Engineering, 63(1), 74–77. (in Chinese)

[15] Tao, S., Yao, H. J., Song, Y. D., et al. (2022). Analysis of supraharmonic generation mechanism of three-phase Vienna charger. Power System Protection and Control, 50(5), 22–32. (in Chinese)

[16] Zhang, Y., Fang, J., Gao, F., et al. (2021). Integrated high- and low-frequency current ripple suppressions in a single-phase onboard charger for EVs. IEEE Transactions on Power Electronics, 36(2), 1717–1729. https://doi.org/10.1109/TPEL.2020.3007771.